Journal of Advanced Research in Applied Sciences and Engineering Technology

Journal homepage:
https://semarakilmu.com.my/journals/index.php/applied_sciences_eng_tech/index
ISSN: 2462-1943

Investigation of Two-Way Fluid-Structure Interaction of Blood Flow at Different Temperature using CFD

Mohsen J. Jweeg[1], Emad Qasem Hussein[2], Farhan Lafta Rashid[2,*], Ali Basem[3]

[1] Aeronautical Technical Engineering, Al-Farahidi University, Baghdad 10011, Iraq
[2] Petroleum Engineering Department, University of Kerbala, Karbala 56001, Iraq
[3] Air Conditioning Engineering Department, Faculty of Engineering, Warith Al-Anbiyaa University, Karbala 56001, Iraq

ARTICLE INFO

Article history:
Received 26 September 2023
Received in revised form 5 November 2023
Accepted 15 November 2023
Available online 30 December 2023

Keywords:

Pulsatile flow; Non-Newtonian fluid; Blood artery; Temperature; CFD

ABSTRACT

At this work, fluid-structure interaction was used to biomechanical challenges relating to blood flow in artery bifurcation to investigate potential solutions. The purpose of this study was to evaluate the influence that artery geometry has under constant flow, pulsatile flow, and varied blood temperatures. In this study, the flow of blood through the artery was simulated using a non-Newtonian fluid model, and the finite element technique was utilized to analyse the data. For the purpose of analysing the differences between pulsatile flow and steady flow, a user-defined function, or UDF, was developed as part of the suggested input velocity model. In order to accurately estimate the pressure distribution, velocity flow, wall shear stress, and wall deformation, a simulation called ANSYS 17.2 is used to model the fluid-structure interaction that occurs when blood flow is superimposed on an arterial wall. According to the findings, the pressure amplitude steadily increases in the artery zone for high temperatures, demonstrating that the projected pressure is 15% greater than it was when the temperature was low. This is in contrast to the low temperature, for which the predicted pressure was 15% lower. In addition, the area close to the apex has the highest levels of shear stress, which then drop down precipitously farther along the wall until they reach an almost constant level. In general, the location of maximum total deformation is shown at peak systole for the artery when the temperature is high. This is the location where the pressure is high, particularly at the artery bifurcation, and where there is a maximum wall deformation of 0.447 mm. In addition, this is the location where the maximum total deformation occurs. These findings are of great use in the design of arterial bifurcation as well as the assessment of recurrent mechanical loads, both of which contribute to the prediction of life.

1. Introduction

The circulation of blood via the arteries is a complicated process that takes place in three dimensions. During this process, pulsating fluid moves through a flexible conduit. Because of the flexible nature of arteries, these unsteady loads on the arterial wall cause the wall to move in an

* *Corresponding author.*
E-mail address: farhan.lefta@uokerbala.edu.iq

https://doi.org/10.37934/araset.36.2.120130

unstable way. They also contribute to the normal and tangential stresses that are placed on the arterial wall. From a clinical point of view, the majority of published papers on blood flow consider the artery as if it were a hard wall. The magnitude and variance of the stresses at the endothelium/blood interface are of interest because of their putative significance in thermogenesis [1]. Because the cause and development of many arterial diseases that lead to the malfunction of the cardiovascular system are, to a great extent, related to the flow characteristics of blood in conjunction with the geometry of the blood vessels, the study of blood flow through arteries is very important. This is because of the fact that the cause and development of many arterial diseases leads to the malfunction of the cardiovascular system [2].

The assumption of rigid walls is made in large part due to the difficulty of finding a solution to the problem of coupled blood flow and vessel deformation. This assumption is justified by the observation that, under normal conditions, wall deformability does not significantly alter the velocity field, this finding was established for arteries where the wall motion is minimal; it is possible that this observation may not hold true for arteries where the deformations are greater [2]. The modelling of the three-dimensional blood flow in compliant arteries, which are tethered to and supported by the surrounding tissue and organs, is extremely difficult for a number of additional reasons. Some of these reasons include the necessity of precise constitutive descriptions of the behaviour of the tissue and outflow boundary conditions. In order to apply methods of fluid–structure interaction in simulation-based medical planning, additional work must be done because multiple surgical interventions need to be modelled, solved, analysed, and compared within a timeframe that is relevant to clinical practice [3,4]. This can be a challenging endeavour.

Blood's nature and behaviour are not only dependent on the fluid's properties, but also on other mechanical factors, such as the forces that are exerted on the fluid, the fluid's motion, and the boundary conditions of the arterial geometry. These factors all work together to determine blood's nature and behaviour. In addition to this, the viscosity of the blood also controls its behaviour. The flow of blood may be described as either being constant or pulsatile, Newtonian or Non-Newtonian, laminar or turbulent, depending on which of these characteristics are present. It is possible to characterize fully developed flows using velocity and pressure fields, with all kinematic parameters being independent of the axial coordinate; however, this ideal behaviour is never realized in the vascular system [5]. There are two key distinctions that can be made between the wall of a blood artery in the vasculature and the materials that are often used for constructing pipes. In contrast to pipes, which typically have a stiff structure, the walls of blood vessels are both elastic and porous [6].

The modelling and simulation of how blood flows through an artery is an important technical challenge. The objective of this study is to do a CFD simulation on a non-Newtonian model of blood. In order to make an accurate prediction of the interaction that occurs between the flow of blood and the elastic walls of the blood vessel while carrying out numerical simulations on different arterial blood temperatures for pulsatile flow. After running the simulation, we are able to witness the pressure and velocity contours that are present within the wall. In addition, we are able to investigate the stresses and deformations that are present in the wall as a result of the force that is applied by the blood. Therefore, it has the potential to improve the effectiveness of contemporary medical therapy.

2. Geometry and Boundary Conditions

ANSYS Design Modeller is used to create the geometry of the fluid domain, and ANSYS Meshing is used to construct the computational grid. A bifurcating artery with a length of 12.5 centimetres and a wall thickness of t=0.5 millimetres; blood enters the bifurcating artery from the inlet and leaves

by either of the two outputs; this is seen in Figure 1. The diameter of the artery at its entrance is around 7 millimetres. The diameter of outlet number one is around 7 millimetres, whereas the diameter of outlet number two is approximately 5 millimetres.

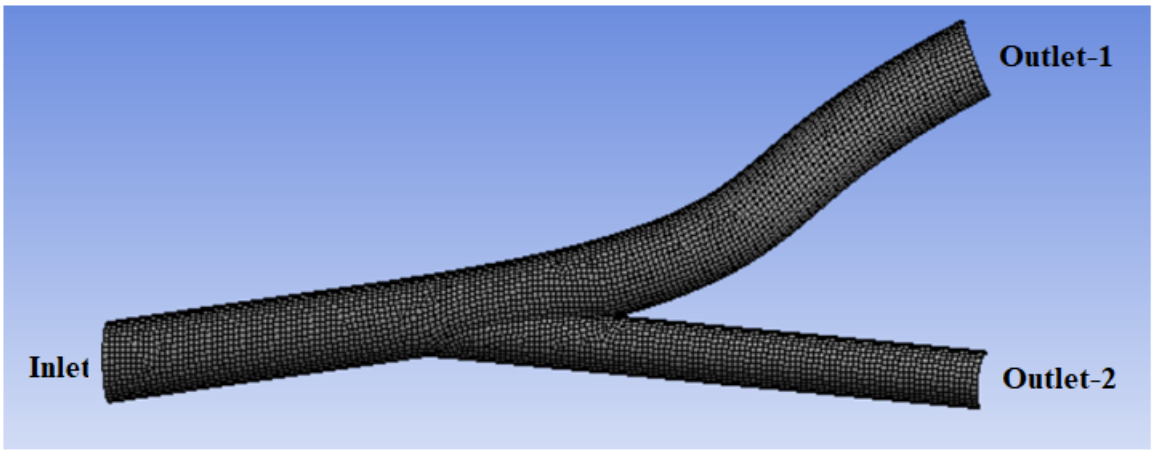

Fig. 1. Geometry model of 3D bifurcation artery in blood region

Blood was confused with a fluid that is homogeneous and incompressible and has the qualities of blood that are outlined in Table 1.

Table 1
Elastic properties of artery blood at normal temperature [7,8]

Physical properties	Value
Density, $\mathrm{kg/m^3}$	1060
Young modulus, MPa	1.08
Poisson ration	0.49
Thermal conductivity, W/m.K	0.492
Specific heat capacity, J/kg.K	3594

Because blood is a non-Newtonian fluid, its viscosity coefficient is not a fixed value; rather, it varies according on the temperature, as shown in Table 2. This relationship may be shown by referring to the table.

Table 2
Parametric variation of viscosity with temperature [8]

Case	Temperature (K)	Blood viscosity(Pa.s)
1	312	$2.689 * 10^{-3}$
2	309	$3.00 * 10^{-3}$
3	295	$3.784 * 10^{-3}$

The fluid domain is given the boundary conditions of having a time-dependent entrance velocity and a constant pressure of 100 mm Hg at the outflow. These conditions are imposed as the applied boundary conditions. The walls of the artery models are presumed to have some degree of flexibility. In the case of a study flow, the velocity at the inlet was maintained at 0.3 meters per second throughout the experiment, and a pulsatile flow sinusoidal profile of inlet velocity throughout artery was utilized to imitate a physiological pulse (see Figure 2 for an illustration of this). In order to

implement the suggested inlet velocity model, a user-defined function, or UDF, was penned [9-11]. In the ANSYS software, further information about boundary conditions will be presented.

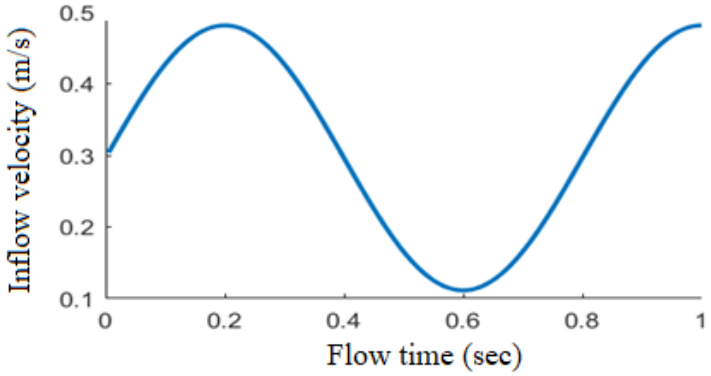

Fig. 2. The sinusoidal pulsatile flow profile of non-newton fluid

3. Mathematical Model

The simulation is executed with the help of the ANSYS 17.2 program coupling function that is available with the company's ANSYS Workbench package. Both the continuity equation and the Navier–Stokes equations, which may be written as follows [12,13], are considered to be the general differential equations of motion that are responsible for regulating the flow of incompressible fluids.

$$\nabla . V = 0 \tag{1}$$

The Navier–Stokes equations have the inertia forces listed on the left-hand side of the equation. These forces are balanced off by the forces listed on the right-hand side of the equation, which include the pressure force, the body force, and the viscous force;

$$\rho \left(\frac{\partial V}{\partial t} + V . \nabla V \right) = -\nabla P + \rho g + \mu \nabla^2 V \tag{2}$$

Where stands for the density of the fluid, V=u,v,w for its velocity in the x, y, and z directions, g for the acceleration of the gravitational field vector, for the fluid's viscosity, and P for its pressure. The pressure–velocity coupling in the existing three-dimensional laminar CFD model may be achieved by utilizing the SIMPLEC method. This simulation makes use of a spatial discretization technique to discretize equations such that they may be solved by a solver that is a second-order upwind. The Green–Gauss cell-based scheme and the PRESTO pressure scheme are both used in the application of the transient simulation scheme, which is a first-order implicit scheme. This scheme is implemented in time. In order to simplify the basic equations and get a better approximation of the features of the domain's blood flow, one might make a number of assumptions. The individual components of the stress tensor, which are denoted by the equation for the constitutive property as [14,15];

$$\sigma_{ij} = -P\delta_{ij} + 2\mu e_{ij,} \qquad i,j = 1,2,3 \tag{3}$$

In Eq. (3) above, δ_{ij} the Kronecker delta,$\mu$is the dynamic viscosity and e_{ij}=1,2,3 are the components of the strain rate tensor defined as follows;

$$e_{ij} = \frac{1}{2}\left(\frac{\partial u_i}{\partial x_j} + \frac{\partial u_j}{\partial x_i}\right) \quad (4)$$

4.Verification and Validation

For the purpose of this simulation of blood flow in 3D arteries, the majority of the physical qualities have been accounted for. These include the non-Newtonian fluid properties of blood as well as the pulsatile aspect of the flow. Elastic wall elements, on the other hand, need to be included into the simulation in order to get it as near as possible to the actual situation. By linking the solution from the FEA simulation with the CFD simulation in ANSYS Workbench, it is possible to achieve this goal. In this particular instance, we will examine the inlet boundary conditions to confirm that the UDF is functioning as we had anticipated it to. After that, we will do a mesh refinement and make use of a lower time step in order to determine whether or not the findings are in agreement with the initial computation [16,17]. By using a finer mesh and a more incremental approach to the time step. Despite the fact that findings were derived from the FSI investigation of healthy pulse oscillations. In this part of the illustration, the maximum pressure that each scenario may exert on the wall is computed. The findings that were achieved after the spatial and temporal refining will then be compared to one another using a case study.

5. Results and Discussion

The ANSYS Fluent tool was used to create the 3D model of the arteries in order to study blood hydrodynamics and shear loads at various temperatures. The impacts of a few blood flow parameters were then investigated for both steady-state and pulsatile flow scenarios. It was done [18-20] to investigate how the arterial's wall shear stresses, flow rate, and pressure distribution changed as the blood temperature changed. The findings of the study's pulsatile flow and velocity flow are shown in Figure 3. It may be argued that the velocity behaviour is comparable in both circumstances, with the differences being negligibly small, since the constant input velocity solution is, on average, smoother than the velocity profiles. Both examples have an identically sized and situated recirculation zone.

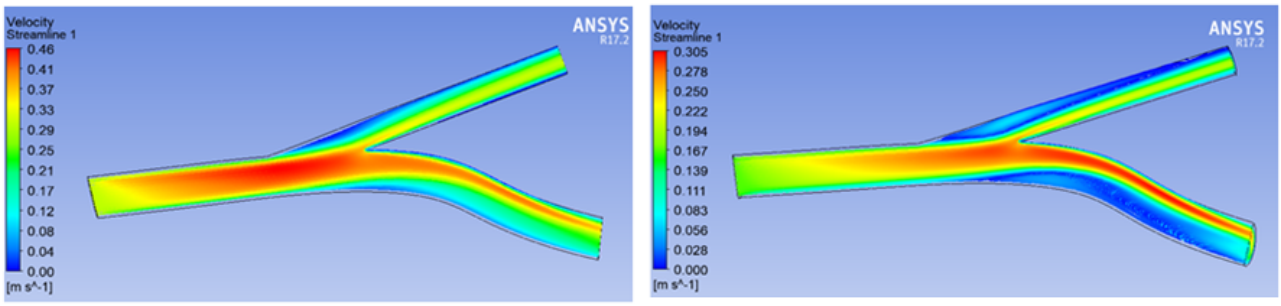

study flow pulsatile flow

Fig. 3. Contour plots of velocity distribution for different inlet velocity (steady and pulsatile)

In Figure 4, the impact of temperature change on blood flow is shown at various temperatures. For the artery, the linear relationship between heat conductivity and blood flow has been verified. Viscous blood moves rapidly and without much trouble when the blood flow is low in viscosity. Due to the elevated blood viscosity, an adverse condition may result in a reduction in blood flow rate. Blood viscosity is thought to decrease by 2% for every 1 °C rise in body temperature. The relationship between flow and viscosity is inverse, and blood is non-Newtonian because circulatory shock causes

it to become more viscous at low flow velocities. As maintaining a consistent and adequate blood flow rate is the primary objective of the blood circulation control system.

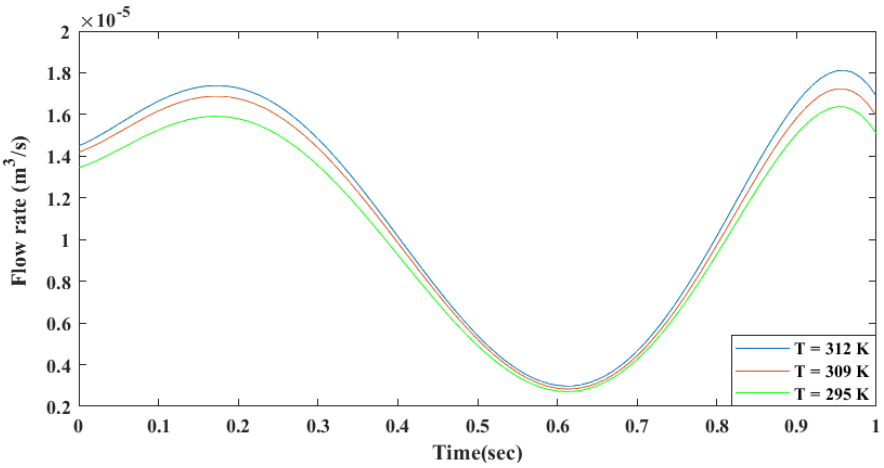

Fig. 4. Blood flow rate with time at different values of the temperature

The findings of the research and pulsatile flow's effects on blood pressure distribution on blood wall are shown in Figure 5. This pressure contour clearly demonstrates that the pressure is greater towards the apex where the flow divides into the daughter branches. Additionally, the artery is squeezed when the gauge pressure is negative due to the pressure differential, which is greater outside the artery and lower within the artery. Furthermore, the pressure contours in the FSI simulations exhibited the same qualitative pattern [21].

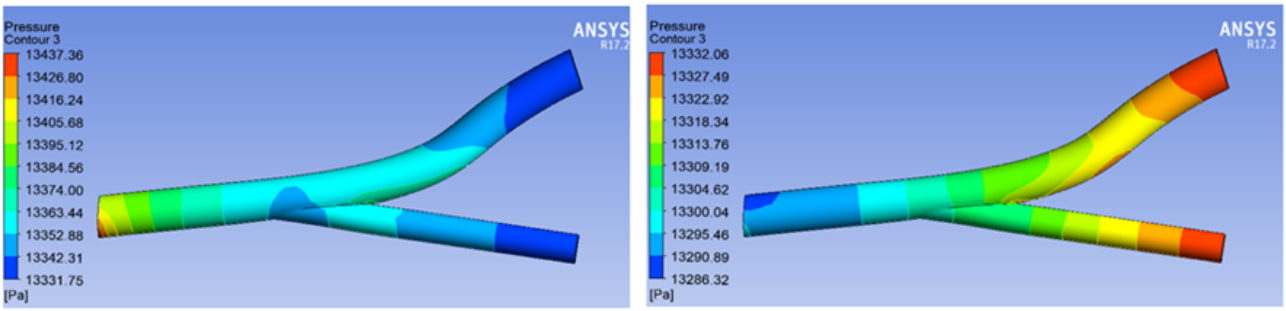

study flow pulsatile flow

Fig. 5. Contour plots of pressure distribution for different inlet velocity (steady and pulsatile)

In order to compare the pressure in various situations, the influence of the blood temperature on the blood wall is shown in Figure 6 at various temperatures. It is shown that at high temperatures, the pressure amplitude gradually increases in the arterial zone. According to the findings, the calculated pressure is 15% greater for the high temperature than the low temperature. The figure's conclusion—a 10.38% rise in pressure as a consequence of a 312 K temperature increase—must have therapeutic significance. Although sensing models for pressure patterns exhibit a similar tendency, there are significant disparities in magnitude, the body may adjust by increasing blood flow.

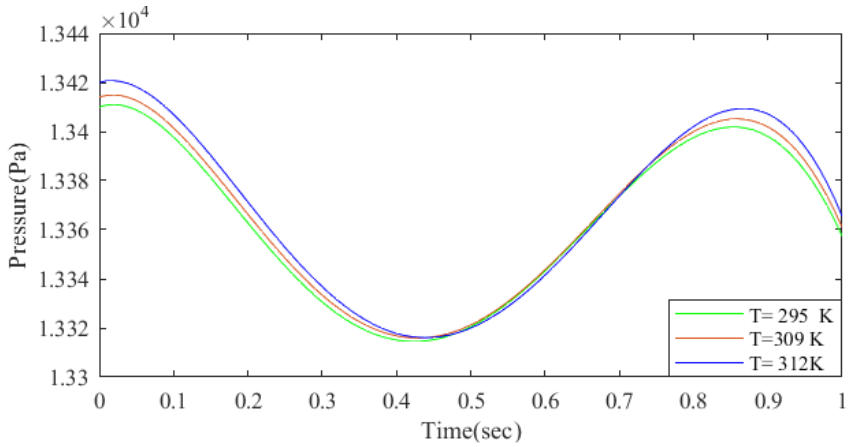

Fig. 6. Blood pressure with time at different values of the temperature

Figure 7 illustrates the shear stress distributions throughout the walls of the artery, which is an essential parameter in the studies of blood flow through arteries. These investigations have demonstrated that shear stress is an important parameter. The position of the WSS drop aligns with a place that is favourable to the emergence of plaque and is compatible with the theory that the recirculation zone is responsible for the phenomenon. At this portion, the maximum wall shear stress reaches 2.1 Pa at its apex. Gradients in the velocity either rose or reduced as a consequence of the beginning or end of the geometry's arterial curvature [22-25]. This was because the geometry included an arterial curvature. The wall of the artery is subjected to strain as a result of the fluctuations in pressure caused by the flow of blood through it.

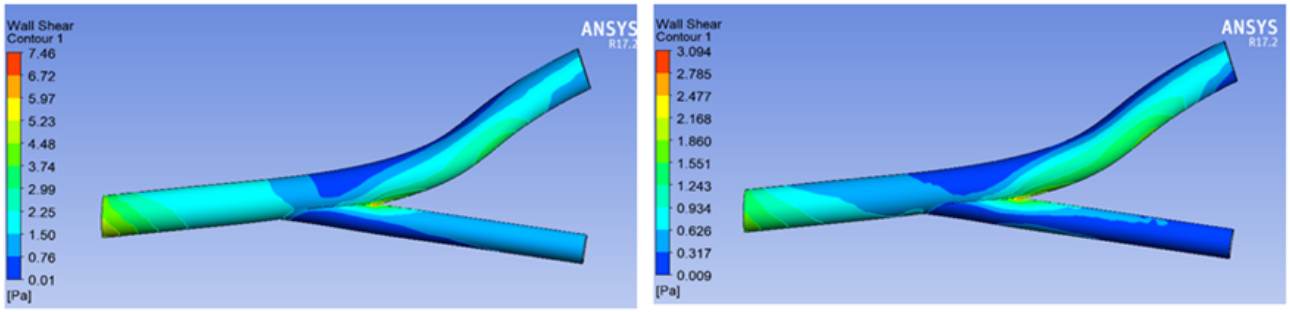

Fig. 7. Contour plots of shear stress on the wall for different inlet velocity (steady and pulsatile)

Figure 8 illustrates the influence that temperature has on shear stress by showing that, for a given amount of temperature, the highest shear stress is localized around the apex area, and then it rapidly decreases down the wall until becoming almost constant again. In addition, the highest value is reached at temperatures below freezing because of an increase in viscosity.

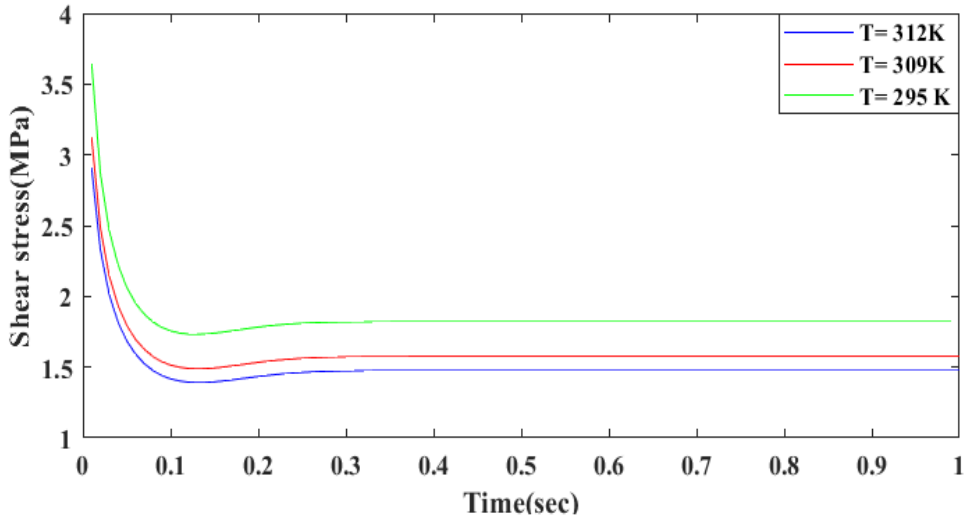

Fig. 8. Shear stress on the wall with time at different values of the temperature

In order to look into the examination of artery bifurcation's strength at various temperatures. ANSYS transient analysis is used to hold the three ends of the artery fixed throughout the FSI. In the cruciform sample, the stress distribution is not uniform, with the largest stresses along the curved edges and the lowest stresses in the centre of the complete model, as seen in Figure 9 and Figure 10. At various temperature field values, stress varies from 6.24 to 8.65 MPa. It indicates that the highest peak value was reduced by 21% due to the large variations in the stress value at the artery's commencement. The pressure field produced by the flow exerts pressure on the artery walls.

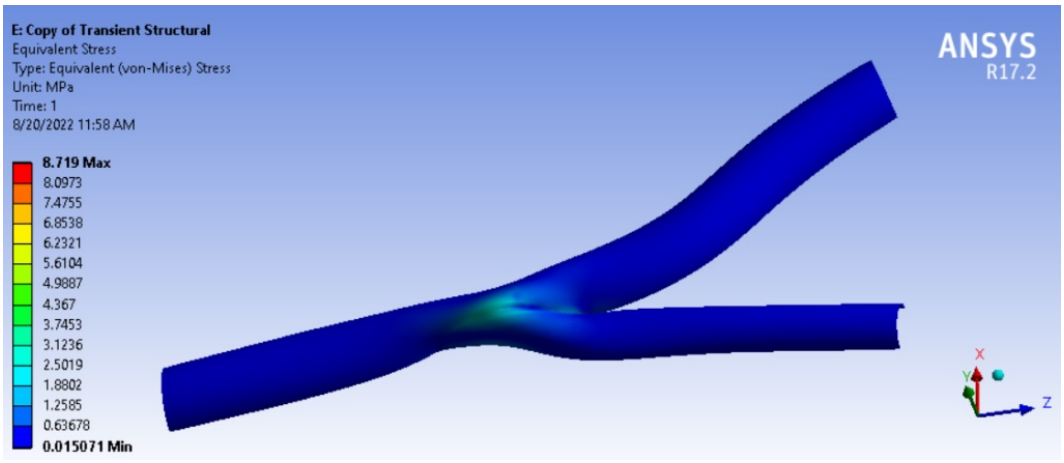

Fig. 9. Contour plots of the Von-Misses stress on the wall in blood temperature 312 K

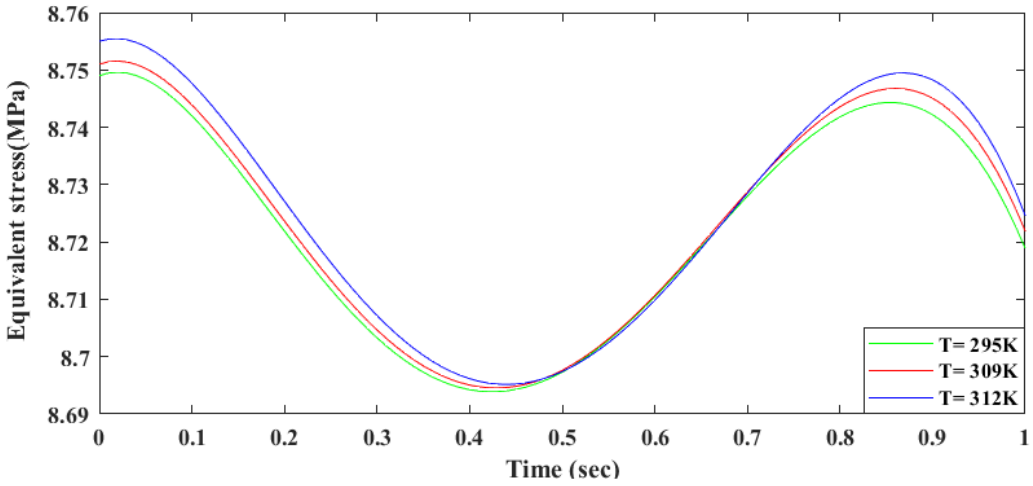

Fig. 10. Von-Misses stress on the wall with time at different values of the temperature

The wall deformation trend's behaviour is identical to that of the whole stress domain and is seen in Figure 11 and Figure 12. Due to the lower arterial stiffness caused by the curvature, the bifurcation zone, namely at the base of the artery branching, has the most deformation. In general, maximal deformation occurs near the pressure's centre, particularly at the bifurcation's apex. The bifurcation's curvature lessens the wall's stiffness, causing a considerable degree of wall deformation to be seen at peak systole for the artery at its warmest temperature (maximum deformation of 0.447 mm, 0.516 mm). The arterial tissue remodelling process is initiated owing to the loss of mechanical strength and stretch of the artery tissue caused by changes in blood pressure. The blood pressure in the artery increases as the simulation goes on, expanding the elastic arterial structure. As a consequence of the fluid barrier expanding, the pressure of the blood flowing through the artery decreases, and the artery is perceived to constrict.

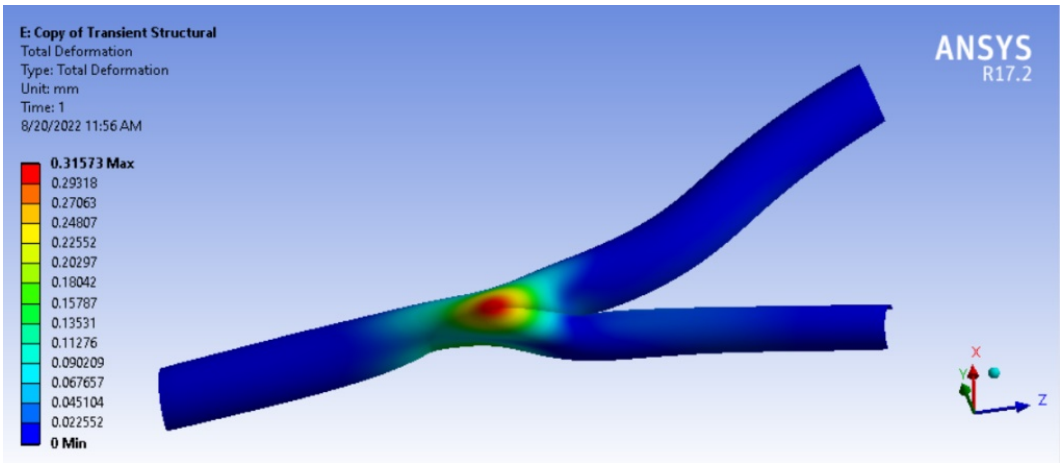

Fig. 11. Contour plots of the total deformation on the wall in blood temperature 312 K

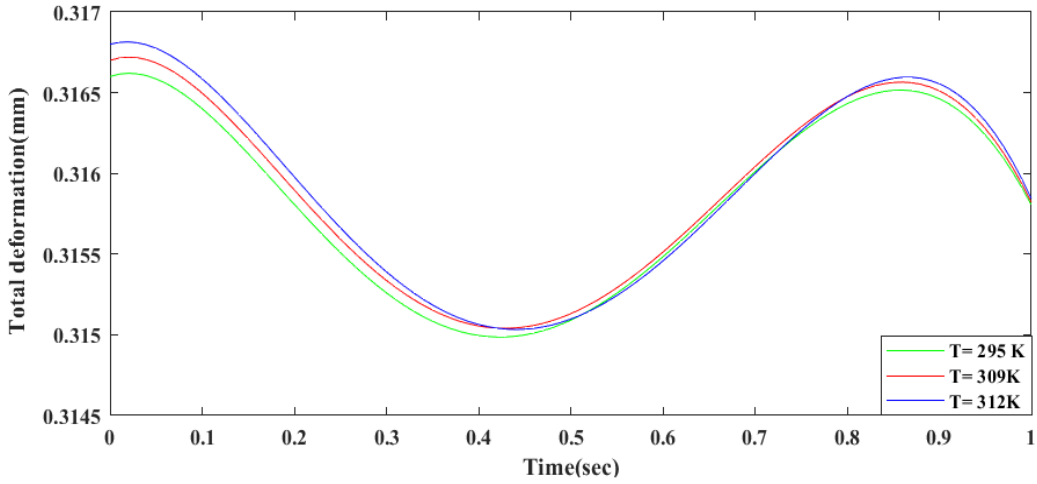

Fig. 12. Total deformation on the wall with time at different values of the temperature

6. Conclusions

ANSYS 17.2 is used to model two-way fluid-structure interaction in blood flow in arteries, and the results are published at various temperature field values. The artery model was based on non-linear elasticity, and the blood was represented as an incompressible fluid. The findings demonstrate that the hemodynamic properties are significantly influenced by the elastic deformation of the wall. For various values of the temperature field, the blood flow rate and negative pressure in the small neck both slightly rose, whilst the wall shear stress marginally reduced. Since whole blood viscosity generally decreases as blood temperature increases, the shear rate is low. However, temperature variations and low-flow conditions have the power to drastically modify it.

Acknowledgement
This research was not funded by any grant.

References

[1] Zhao, X., J. M. T. Penrose, S. Z. Zhao, T. G. Karayiannis, and M. W. Collins. "Numerical study of fluid solid interaction (FSI) in arteries." In *Proceeding of WSEAS and IASME International Conferences on Fluid Mechanics*, pp. 17-19. 2002.

[2] Kumar, Gaurav, Hitesh Kumar, Kabir Mandia, M. Zunaid, N. A. Ansari, and A. Husain. "Non-Newtonian pulsatile flow through an artery with two stenosis." *Materials Today: Proceedings* 46 (2021): 10793-10798. https://doi.org/10.1016/j.matpr.2021.01.697

[3] Deparis, Simone, Miguel Angel Fernández, and Luca Formaggia. "Acceleration of a fixed point algorithm for fluid-structure interaction using transpiration conditions." *ESAIM: Mathematical Modelling and Numerical Analysis* 37, no. 4 (2003): 601-616. https://doi.org/10.1051/m2an:2003050

[4] Gudekote, Manjunatha, and Rajashekhar Choudhari. "Slip effects on peristaltic transport of Casson fluid in an inclined elastic tube with porous walls." *Journal of Advanced Research in Fluid Mechanics and Thermal Sciences* 43, no. 1 (2018): 67-80.

[5] Ilyas, Rushdan Ahmad, Salit Mohd Sapuan, Mohamad Ridzwan Ishak, and Edi Syams Zainudin. "Water transport properties of bio-nanocomposites reinforced by sugar palm (Arenga Pinnata) nanofibrillated cellulose." *Journal of Advanced Research in Fluid Mechanics and Thermal Sciences* 51, no. 2 (2018): 234-246.

[6] Renner, Johan. "Towards Subject Specific Aortic Wall Shear Stress: A Combined CFD and MRI Approach." PhD diss., Linköping University Electronic Press, 2011.

[7] Sriyab, Somchai. "The effect of stenotic geometry and non-Newtonian property of blood flow through arterial stenosis." *Cardiovascular & Haematological Disorders-Drug Targets (Formerly Current Drug Targets-Cardiovascular & Hematological Disorders)* 20, no. 1 (2020): 16-30. https://doi.org/10.2174/1871529X19666190509111336

[8] Çinar, Yildirim, A. Mete Şenyol, and Kamber Duman. "Blood viscosity and blood pressure: role of temperature and hyperglycemia." *American journal of hypertension* 14, no. 5 (2001): 433-438. https://doi.org/10.1016/S0895-7061(00)01260-7
[9] Siddiqui, S. U., N. K. Verma, Shailesh Mishra, and R. S. Gupta. "Mathematical modelling of pulsatile flow of Casson's fluid in arterial stenosis." *Applied Mathematics and Computation* 210, no. 1 (2009): 1-10. https://doi.org/10.1016/j.amc.2007.05.070
[10] Jhunjhunwala, Pooja, Pramod Padole, and S. Thombre. "CFD analysis of pulsatile flow and non-Newtonian behavior of blood in arteries." *MCB: Molecular & Cellular Biomechanics* 12, no. 1 (2015): 37-47.
[11] Paz, Concepción, Eduardo Suárez, Christian Gil, and Adrián Cabarcos. "Numerical simulation of the fluid-structure interaction to evaluate the stress in arteries with atheromas." In *11th National Congress on Experimental Mechanics*, pp. 923-932. 2018.
[12] Kallekar, Laxman, Chinthapenta Viswanath, and Mohan Anand. "Effect of wall flexibility on the deformation during flow in a stenosed coronary artery." *Fluids* 2, no. 2 (2017): 16. https://doi.org/10.3390/fluids2020016
[13] Kanakamedala, Karthik. "Numerical Simulation of the Flow of a Power Law Fluid in an Elbow Bend." PhD diss., Texas A & M University, 2010.
[14] Ma, Jieyan. *Development of Numerical Tools for Hemodynamics and Fluid Structure Interactions*. The University of Manchester (United Kingdom), 2014.
[15] Ponzini, Raffaele. "PRACE Autumn School 2013-Delayed Detached Eddy Simulation of Yacht Sails." (2013).
[16] Li, Mingxiu. "Numerical simulation of blood flow and vessel wall stresses in stenosed arteries." PhD diss., University of Edinburgh, 2006.
[17] Al-Shammari, Mohsin Abdullah, Emad Q. Hussein, and Ameer Alaa Oleiwi. "Material characterization and stress analysis of a through knee prosthesis sockets." *International Journal of Mechanical & Mechatronics Engineering* 17, no. 6 (2017).
[18] Al-Waily, Muhannad, Emad Q. Hussein, and Nibras A. Aziz Al-Roubaiee. "Numerical modeling for mechanical characteristics study of different materials artificial hip joint with inclination and gait cycle angle effect." *Journal of Mechanical Engineering Research & Developments* 42, no. 4 (2019): 79-93. https://doi.org/10.26480/jmerd.04.2019.79.93
[19] Alishahi, M., M. M. Alishahi, and H. Emdad. "Numerical simulation of blood flow in a flexible stenosed abdominal real aorta." *Scientia Iranica* 18, no. 6 (2011): 1297-1305. https://doi.org/10.1016/j.scient.2011.11.021
[20] Nowakowska, Oliwia, and Zbigniew Buliński. "Mathematical modelling of heat transport in a section of human forearm." *Computer Assisted Methods in Engineering and Science* 22, no. 4 (2017): 347-363.
[21] Fluent, A. N. S. Y. S. "ANSYS fluent UDF manual." *ANSYS Inc., USA* (2015).
[22] Degroote, Joris, Abigail Swillens, Peter Bruggeman, Robby Haelterman, Patrick Segers, and Jan Vierendeels. "Simulation of fluid–structure interaction with the interface artificial compressibility method." *International Journal for Numerical Methods in Biomedical Engineering* 26, no. 3-4 (2010): 276-289. https://doi.org/10.1002/cnm.1276
[23] Rashid, Farhan Lafta, Baqer A. Alhabeeb, Mohammed Alhwayzee, and Akeel Abbas Mohammed. "Study the Sudden Expansion and Contraction in the Pipe Line on the Distribution of Pressure at the Presence of a Porous Media by Using CFD Simulation." *Journal of Engineering Science and Technology* 16, no. 5 (2021): 3960-3973.
[24] Fathollahi, Reza, As'ad Alizadeh, Parmida Kamaribidkorpeh, Azher M. Abed, and Pooya Pasha. "Analyzing the effect of radiation on the unsteady 2D MHD Al2O3-water flow through parallel squeezing sheets by AGM and HPM." *Alexandria Engineering Journal* 69 (2023): 207-219. https://doi.org/10.1016/j.aej.2022.11.035
[25] Taher, Rani, Mohamed Mohsen Ahmed, Zoubida Haddad, and Cherifa Abid. "Poiseuille-Rayleigh-Bénard mixed convection flow in a channel: Heat transfer and fluid flow patterns." *International Journal of Heat and Mass Transfer* 180 (2021): 121745. https://doi.org/10.1016/j.ijheatmasstransfer.2021.121745